Composite Structures 310 (2023) 116771

Contents lists available at ScienceDirect

Composite Structures

journal homepage: www.elsevier.com/locate/compstruct

Multi-impact response of semicylindrical composite laminated shells with different thicknesses

P.N.B. Reis [a], P. Sousa [b], L.M. Ferreira [c,*], C.A.C.P. Coelho [d]

[a] Departamento de Engenharia Mecânica. CEMMPRE. Universidade de Coimbra. Pinhal de Marrocos 3030-194 Coimbra. Portugal
[b] Department of Materials Engineering, KU Leuven, Leuven, Belgium
[c] Departamento de Mecánica de Medios Continuos y Teoría de Estructuras. Escuela Politécnica Superior. Universidad de Sevilla. Camino Descubrimientos, S/N 41092 Sevilla. España
[d] Unidade Departamental de Engenharias. Escola Superior de Tecnologia de Abrantes. Instituto Politécnico de Tomar. Rua 17 de Agosto de 1808 S/N 2200-370 Abrantes. Portugal

ARTICLE INFO

Keywords:
Composite materials
Semicylindrical shells
Low-velocity impacts, Mechanical testing
Damage analysis

ABSTRACT

Nowadays, composite materials are increasingly used in the most diverse areas of engineering, where non-planar geometries begin to be quite frequent. However, the existing knowledge about its mechanical performance is still not enough for structural applications. Therefore, experimental tests were carried out to study the thickness effect on static compression and multi-impact response of laminated E-glass/Polyester semicylindrical shells. For this purpose, specimen with thicknesses of 1.1 mm, 1.6 mm and 2.1 mm (corresponding to 6, 9 and 12 woven fabric layers) were considered. In terms of static response, higher thicknesses are responsible for higher compressive strength and stiffness, reaching, in the first case, differences of 252.6 % between the thinnest and thickest shells. Regarding the multi-impact response, the impact fatigue life increases 17.4 times for the analysed thickness range, which can be explained by the different damage mechanisms observed. It was observed that impact damage becomes more localized with increasing thickness, because the energy is dissipated by more interfaces.

1. Introduction

Composite material structures are often submitted to low and/or high-velocity impact loads. An aircraft, for example, can experience impact loads due to a falling tool during maintenance, the projection of debris from the runway during the take-off or landing, or bird impacts. These types of events cause very localised damage with high-stress concentrations around the impact point.

The sequence of events in impact damage can be classified into two stages: appearance of microcracks in the matrix and respective propagation to a neighbouring interface leading to delamination [1]. In a localised impact, the energy is dissipated by the elastic deflection, deformations due to contact, fracture mechanisms, stress propagation, vibrations, and inertia [2]. However, for low-velocity impacts, the first three forms are preponderant and at the level of damage mechanisms, the main failure modes are matrix cracking, delamination, fibre failure and perforation [3–8]. In terms of delaminations, it is recognized that different bending stiffnesses between adjacent layers with different orientations are decisive for their triggering [9], but they only occur in presence of matrix cracking and after a certain amount of failure energy, below which, the energy is absorbed in the elastic regime of the composite laminate [5,10,11]. Therefore, under these conditions, the delaminated area increases with increasing the difference between the orientations of adjacent layers [6,10,12,13].

The low-velocity impact phenomenon has been extensively studied and conveniently reported in the bibliography for planar geometries (plates), but for non-planar geometries (such as curved, cylindrical, and spherical shells) the available literature is still scarce. Basically, the published works focus on numerical and experimental studies reporting the influence of geometric parameters, boundary conditions and different materials/lay-up configurations on the impact response of semicylindrical composite laminates. For example, the influence of thickness and radius of curvature of semicylindrical composite laminates was studied in [14–21], and it was concluded that increasing thickness promotes an increase in stiffness and, consequently, higher impact loads and smaller deflections and contact times are obtained

* Corresponding author.
E-mail addresses: paulo.reis@dem.uc.pt (P.N.B. Reis), pedro.sousa@kuleuven.be (P. Sousa), lmarques@us.es (L.M. Ferreira), cccampos@ipt.pt (C.A.C.P. Coelho).

https://doi.org/10.1016/j.compstruct.2023.116771
Received 16 August 2022; Received in revised form 20 December 2022; Accepted 3 February 2023
Available online 8 February 2023

[15,17,21]. It was also observed that larger curvature radius lead to higher stiffness values, which translates into increased load and decreased contact time [15,16,19–21]. This behaviour of cylindrical shells was object of analysis by Kistler [21]. The author stated that this behaviour may be explained by considering the large deformation response of a cylindrically curved panel under a centrally applied point impulsive load with focus on the stiffness relaxation exhibited in the force–deflection response, which for some cases is like the dynamic stability phenomenon observed in thin, shallow, clamped, spherical shells. However, the curvature has less influence on the impact load magnitude and damage size than the variation in impactor's mass or impact velocity [14,18].

The effect of boundary conditions was studied in [1,15,22,23] and it was observed that both simply supported and fixed ends promote very similar impact loads up to the peak load, from which it changes. The use of fixed ends increases the stiffness of the composite laminate regardless of the curvature, and the damage is higher with increasing curvature. This behaviour is detailed in the study by Kistler and Waas [15] where large deformations curved quasi-isotropic panels subjected drop weight impact tests were investigated for simply supported or clamped boundary conditions.

Previous studies were performed by the authors in which the single impact and static response of semicylindrical composite shells was evaluated [24,25]. The hybridisation effect (laminate composite shells composed by different types of fibres), and the thickness effect on carbon composite sandwich cylindrical shells incorporating a cork core were studied in [24] and [25], respectively. It was observed that the impact performance and the compressive static strength are significantly affected by the shellś configuration and that increasing the thickness of shell results in higher values of impact load and stiffness, while the displacement decreases. The effect of the distance between neighbour impacts on semicylindrical composite shells was studied in [26] and it was observed that there is a critical distance beyond which there is no influence on the impact fatigue life.

From this literature review, it is noted that most of the existing studies only address the thickness effect on single impacts. Therefore, the main goal of this study is to investigate the thickness effect on the multi-impact response of composite semicylindrical shells. For this purpose, experimental tests were carried out using semicylindrical shells with three different thicknesses. The results will be discussed based on typical curves obtained from these tests and, according to the authors' knowledge, there are still no studies in literature involving repeated impacts on composite semicylindrical shells dedicated to. Finally, each configuration was subjected to a static compression analysis and the residual strength evaluated after a certain number of impacts.

2. Material and experimental procedure

Composite laminate semicylindrical shells were produced by hand lay-up with dimensions and mould shown in Fig. 1. For this purpose, an AROPOL FS 1962 polyester resin and a MEKP-50 hardener were used, a system that was reinforced with bi-directional E-glass woven fabric (taffeta with 210 g/m^2). More details about the resin can be found in [27]. Semicylindrical shells with different thicknesses (t) were produced. It was considered t = 1.1 mm, 1.6 mm, and 2.1 mm (with a standard deviation of 0.06 mm), which correspond to 6, 9 and 12 woven fabric layers, respectively.

After the impregnation phase, the system was placed inside a vacuum bag and subjected to vacuum for 4 h with a maximum pressure of 0.5 mbar to eliminate any air bubbles existing in the composite, as well as to maintain a constant fibre volume fraction and a uniform thickness. Finally, the semicylindrical shells were cured for 24 h at 40 °C and, subsequently, cut to 100 mm in length to obtain the specimens used in the experimental tests. Given the manufacturing (vacuum process) and curing process employed, the springback effect was measured and no significant changes were observed (less than 1 % variation). The cuts were performed with a diamond saw with controlled speed and feed to minimize delamination in the specimens.

Low-velocity impact tests were carried out using a drop weight testing machine IMATEK-IM10. More details of the impact machine can be found in [23], and an impactor diameter of 10 mm with a mass of 2.826 kg was used. According to Fig. 2, the specimens were free supported on the curved edges and the straight edges were simply supported. The impact tests were supported by ASTM D7136 standard and using a previously selected 5 J energy to promote visible damage, but without perforation of the specimens. Notice that perforation occurs when the impactor completely passes through the specimens. The impact load, the displacement and the absorbed energy results were directly obtained from the testing machine, and the IBS was calculated from the impact load–displacement curves. Notice that the IBS is defined by the slope of the ascending branch of the load–displacement curve [28], proving to be an essential tool for evaluating the damage resistance of a composite [28,29].

Finally, the static compressive strength for different configurations was obtained using a universal testing machine Shimadzu AG-100, with the same support and impactor used in the low-velocity impact tests. A displacement rate of 3 mm/min was used, and the displacement values were obtained directly from the crosshead displacement, which is

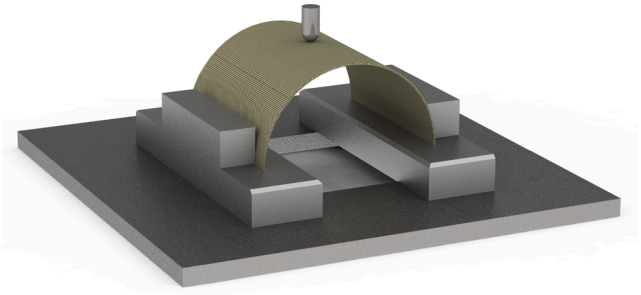

Fig. 2. Schematic representation of the supports used in the experimental tests.

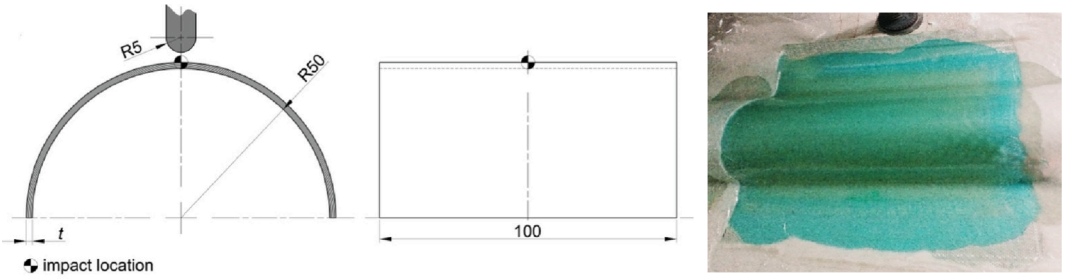

Fig. 1. a) Geometric parameters of the specimens and of the impactor. b) Mould used to obtain the semicylindrical shape.

automatically measured by the testing equipment with an accuracy of ± 0.01 mm.

The impact and static tests were performed at room temperature. Three specimens were experimentally tested for each configuration (6, 9 and 12 layers) for both the impact and the static tests, which corresponds to a total of 18 tested specimens.

A representation of the support used in the experimental is shown in Fig. 2.

3. Results and discussion

3.1. Static characterization

The static performance of semicylindrical composite laminates was obtained by compression tests, and Fig. 3 shows the typical load–displacement curves obtained for the different thicknesses analysed. It is possible to observe that increasing the thickness promotes higher collapse loads and longer linear regimes. For example, thicknesses of 1.1 and 1.6 mm lose linearity for displacements higher than 1 mm, while for 2.1 mm this value is around 4 mm. In addition, increasing the thickness also increases the stiffness of the shells.

The maximum average loads obtained from the curves shown above are illustrated in Fig. 4. Symbols represent the average values, while the dispersion bands represent the maximum and minimum values obtained in each condition. It is possible to notice that for a thickness of 1.1 mm the collapse load occurs for values of 252 N and for 2.1 mm it reaches 889 N, which corresponds to an increase of around 252.6 %. According to the results presented, it is also visible that the increase in compressive strength is linear and capable of being modelled by the mathematical equation expressed in Fig. 4.

Finally, the damage evolution was also analysed and is shown in Fig. 5 for the different thicknesses. It is possible to observe that the damage starts in the region under the indenter and in the upper layers, propagating later along the fibres and towards the edges. After reaching the edges, the saturation of the damage leads to its propagation in the perpendicular direction and from the region where the load is applied. It is also possible to observe that increasing the shell thickness does not significantly alter the damage morphology. In this case, new damages appear parallel to the first ones (along the fibres and towards the edges) and when those propagating in the perpendicular direction reach a certain saturation. When the new damages reach the edges of the specimen, the stiffness drops drastically and, consequently, the collapse is immediate.

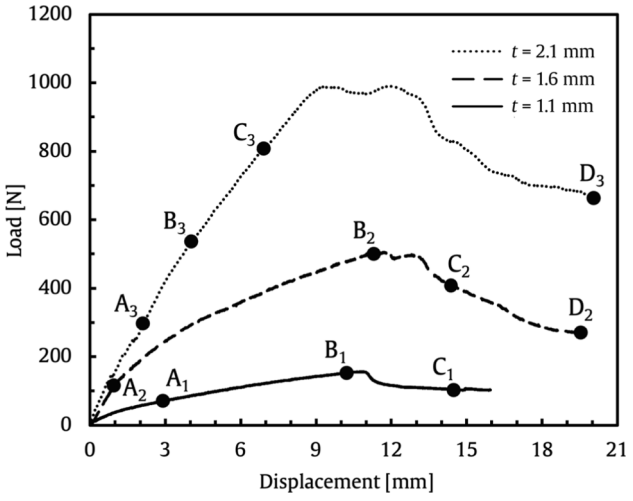

Fig. 3. Typical load–displacement curves obtained for different thicknesses.

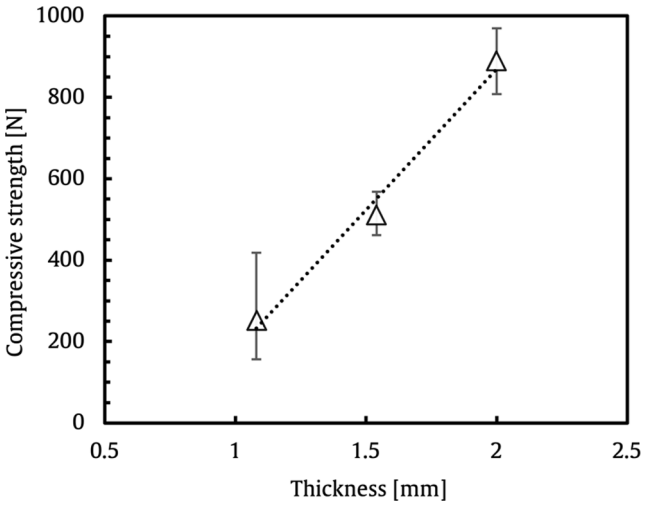

Fig. 4. Compressive strength versus thickness.

3.2. Multi-impact response

The semicylindrical composite laminates were submitted to low-velocity impact tests to evaluate the effect of thickness on the impact strength. Representative load-time and energy-time curves obtained from the experimental tests are shown in Fig. 6, which are in agreement with literature [30–32]. These curves contain oscillations that result from the elastic wave and which are created by the vibrations of the samples [33,34].

From the load-time curves it is possible to observe that the load increases up to a maximum value (P_{max}) followed by its decrease after the peak load. Although this behaviour can be observed for all the configurations, a more detailed analysis of the curves shows that for the specimens with 6 and 9 layers, immediately after reaching the P_{max}, present a sudden drop of the load. This behaviour is a manifestation that a major damage occurs in these thinner specimens. This can be also observed in Fig. 7, where the severity of the damage induced by a single impact is presented for each of the configurations.

Regarding the energy-time curves, it can be noticed that the impact energy used was not high enough for full perforation, because the impactor hits the specimen and returns through rebound. In these curves, the beginning of the plateau corresponds to contact loss between the impactor and the specimen, and the difference between the maximum energy and the energy defined by the plateau is the restored (elastic) component due to impactor rebound [35–37]. Furthermore, when comparing the energy-time curves, it is possible to observe that higher thickness values promote higher restored energy and, consequently, higher amount of absorbed energy leads to larger internal damage. Fig. 7 shows, for example, the failure surface for the various configurations.

It is possible to observe that both size and shape of the damage depend significantly on the thickness, which agrees with the studies developed by Reis et al. [25]. For example, the thinner shells ($t = 1.1$ mm) show damage along the entire length of the shell, starting at the impact region, as well as additional damage in regions further away from the impactor/shell contact zone. For specimens with intermediate thickness ($t = 1.6$ mm), the damage is very similar to that observed in thinner shells, but with less severity. In both cases, cracks in the matrix are followed by delamination under the impact point [14,18], which propagates later towards the edges. Finally, for thicker plates ($t = 2.1$ mm), the damage is localized and confined to the impact point. This analysis shows that higher thicknesses are responsible for smaller areas of damage, which is explained by the smaller displacements observed. According to Zhao and Cho [16], the damage size is related to the total dynamic deformation. Studies developed by these authors also reveal

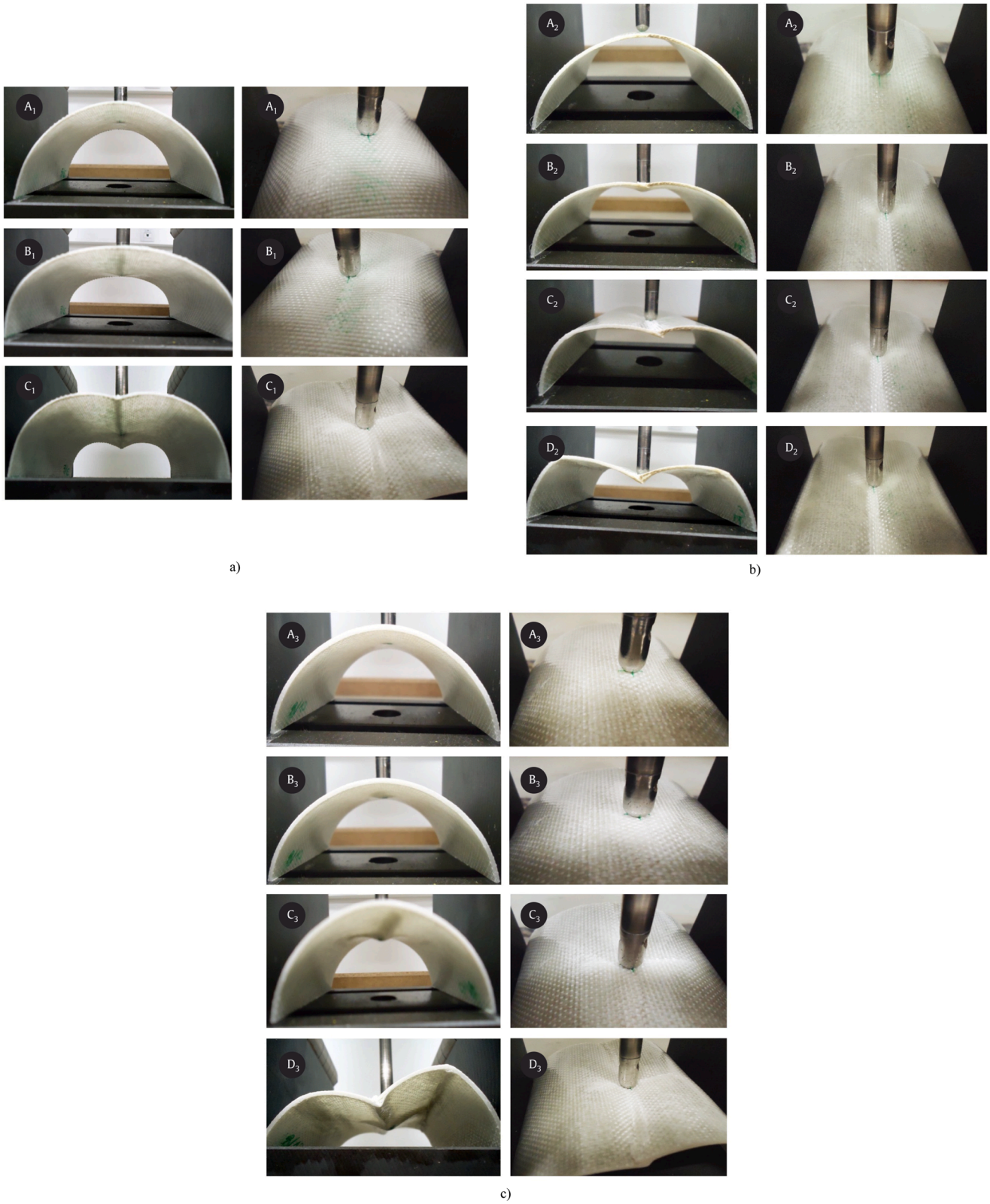

Fig. 5. Damage evolution obtained for the different thicknesses: a) $t = 1.1$ mm; b) $t = 1.6$ mm; c) $t = 2.1$ mm.

that, compared to flat plates, the damage size is smaller and its position changes from the lower interface to the upper interface [19]. The damage first appeared at the top ply and then spread to the bottom layers, although the maximum damage area is on the upper surface (under the point of impact). Moreover, increasing the thickness leads to more interfaces capable of dissipating the impact energy and, consequently, less energy available to increase the damage (i.e., lower damage area). Finally, Kumar [20] observed that matrix cracks essentially occur in the fibre direction.

Therefore, the thickness proves to be an important parameter in the

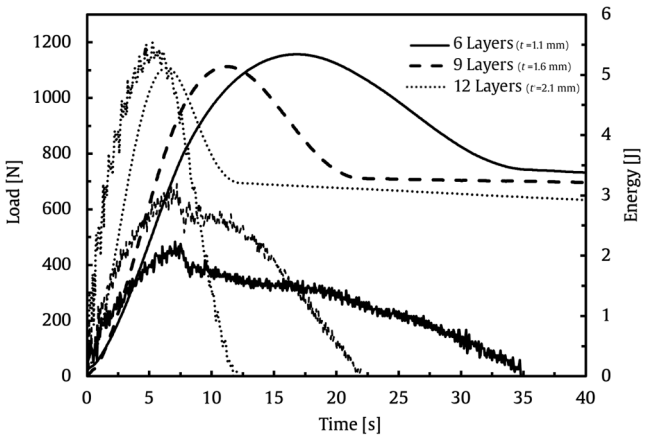

Fig. 6. Impact load-time and energy-time curves for the first impact.

impact response and, according to García-Castillo et al. [38], it is even one of the main parameters that determine the impact properties. In this context, a more detailed analysis is carried out at level of maximum load, maximum displacement, and impact bending stiffness for the first impact, based on the curves shown in Fig. 3. Fig. 8 shows, for example, the thickness effect on the average load and maximum displacement, where the scatter bands represent, respectively, the maximum and minimum values obtained for each condition.

It is possible to observe that for the range of thicknesses studied, the maximum impact load and maximum displacement (deflection) present a linear behaviour. In terms of maximum load, it increases with increasing thickness and the opposite occurs for maximum displacement. For example, for $t = 1.1$ mm the maximum impact load is about 487 N and for $t = 2.1$ mm it reaches 1171 N, which represents an increase of about 140 %. Regarding the maximum displacement, these values are 25.5 mm and 12 mm, respectively, which represents a decrease of 52.9 %. These results are in agreement with several studies available in the literature, which are justified by the increase in stiffness [15–17,21]. Kistler [21], for example, observed that stiffer structures present higher impact strength, lower deflection/displacement, and shorter contact time, while Kistler and Waas [15] and Arachchige et al. [17,39] found that the impact load increases with increasing thickness and the maximum displacement and contact time decrease. Finally, for a better understanding of the stiffness effect on the analysed parameters (maximum load and maximum deflection/displacement), Fig. 9 shows the evolution of the impact bending stiffness (IBS) against thickness.

From this figure it is possible to confirm the increase in stiffness with increasing thickness. For example, for thicknesses of 1.1 mm and 2.1 mm the IBS is 31.3 N/mm and 122.6 N/mm, respectively, which represents an increase of 291.7 %. In addition, it is also possible to observe that this increase in stiffness, for the studied thickness range, follows a second-order polynomial curve. On the other hand, the damage severity observed in Fig. 7 also confirms that IBS can be related to the damage induced by the impact load.

In terms of multi-impact response, Fig. 10 plots number of impacts to failure (Nf) versus thickness, a representation similar to that used in fatigue analysis (SN curves). Mean curve fitted to the experimental results is also superimposed. Collapse was defined when full perforation occurs, which is defined when the impactor completely passes through the samples. Notice that the values in brackets stand for the number of specimens that suffered full perforation for the considered impact

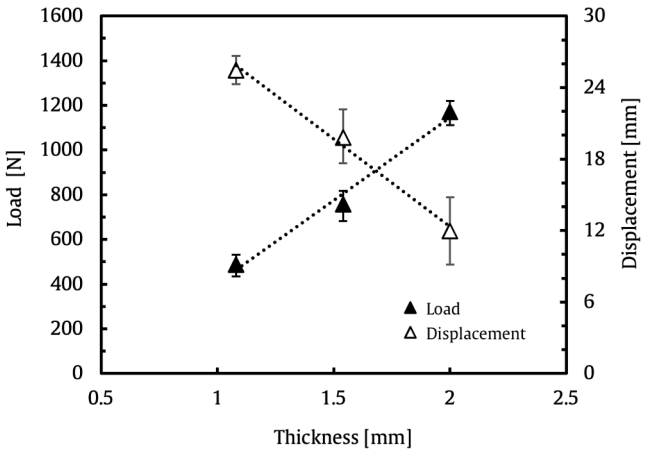

Fig. 8. Maximum impact load and maximum displacement after the first impact for different thicknesses.

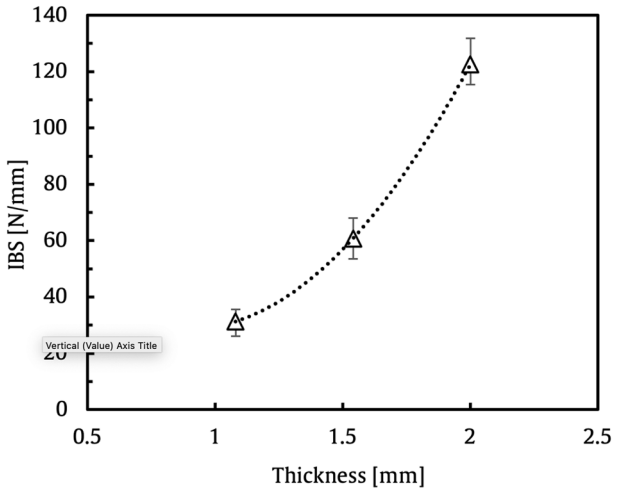

Fig. 9. Impact bending stiffness (IBS) after the first impact for different thicknesses.

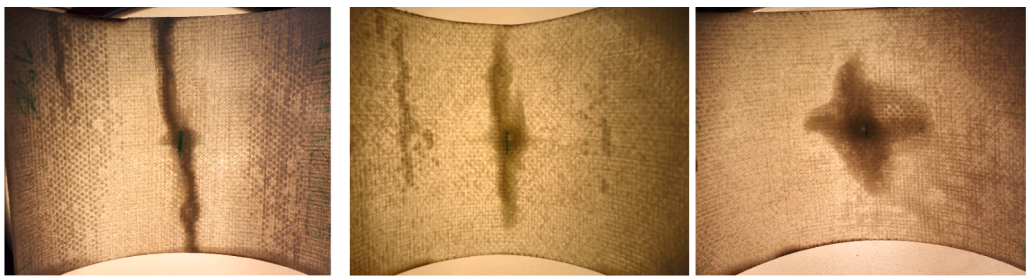

Fig. 7. Damage after the first impact for: a) $t = 1.1$ mm; b) $t = 1.6$ mm; c) $t = 2.1$ mm.

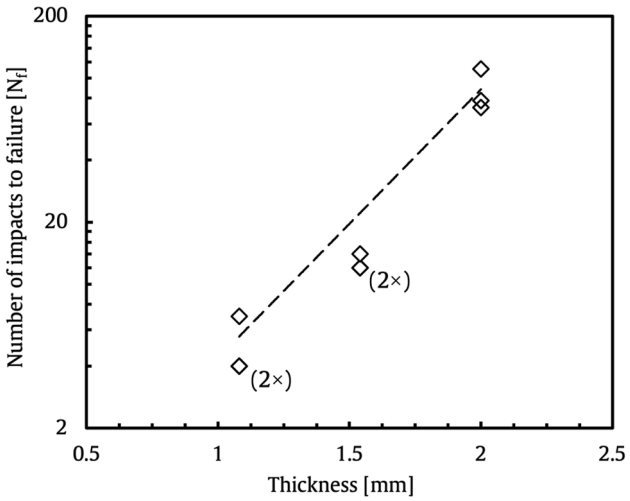

Fig. 10. Number of impacts to failure for different thicknesses.

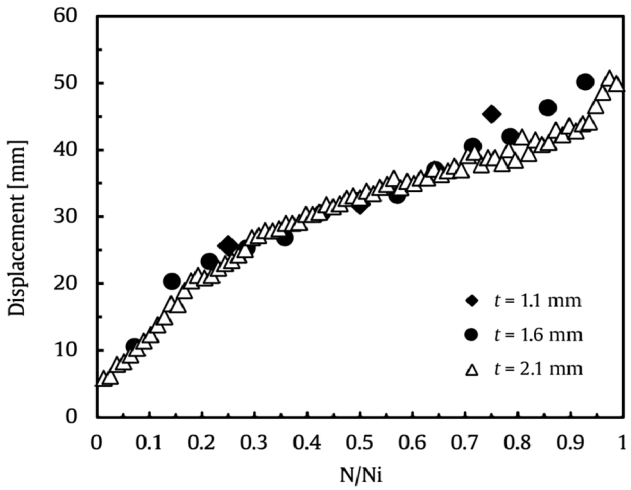

Fig. 12. Evolution of maximum displacement for different thicknesses.

energy level.

As expected, it is possible to observe that higher thicknesses lead to longer lives. For example, in terms of average values, full perforation occurs after 5 and 87 impacts for thicknesses of 1.1 mm and 2.1 mm, respectively. In this case, the impact fatigue life increases by 17.4 times, which can be explained by the different damage mechanisms resulting from the different thickness values. As mentioned above, increasing thickness increases the number of interfaces and, consequently, increases the dissipated energy [20].

To have a better understanding of the multi-impact response, impact parameters will be focus of a more detailed analysis. In this context, for example, Fig. 11 presents the impact load evolution with the multiple impacts for the different thicknesses. N is the number of impacts for a given time and N_f is the number of impacts for which failure occurs. In this representation, the last impact is not shown because full perforation has occurred.

The impact load evolution is very important because it represents the value that the composite can tolerate before undergoing major damage [25,30]. Therefore, as expected, the impact load decreases with the increasing number of impacts due to damage accumulation [40–44]. Consequently, as shown in Fig. 12, the displacement increases. In fact, the accumulation of damage is responsible for lower stiffness values, mainly at the point of impact [40,42,44], which explains the decrease in maximum load and the increase in displacement observed. However, when fibre breakage begins to occur, there is a drastic decrease in stiffness and the variation of these parameters is drastic until final failure. Therefore, typical profiles are expected for these two parameters (impact load and displacement) which, as shown in Figs. 11 and 12, evolve inversely with each other. In both cases, due to the severity of damage [43–45], the experimental data can be fitted by a polynomial of order two for the smallest thickness (1.1 mm), while for 1.6 mm and 2.1 mm they are fitted by a polynomial of order three.

Analysing in detail the evolution of the impact load, and excluding the thinnest shells, the first stage represents the first 30 % of the impact fatigue life and is characterized by a very fast decrease in load due to occurrence of the first damages (cracks in matrix and delamination/interlaminar fracture) and their propagation. It is also noted that a higher thickness leads to a more expressive drop in the impact load during this regime. Subsequently, the second stage extends up to 80 % of the impact fatigue life and is characterized by the saturation of damage initiated in the previous stage, as well as the emergence of new ones. At this stage, the impact load decreases almost linearly with the number of impacts. Finally, the third stage is again characterized by an abrupt drop in load due to high severity of the damages introduced.

Literature reports a strong dependence between these two parameters (impact load and displacement) and stiffness [40], evidence that can be proven by the evolution of the IBS shown in Fig. 13.

It is possible to observe that, similar to the impact load evolution, the IBS values obtained for shells with thicknesses of 1.6 mm and 2.1 mm also present a profile that can be characterized by having three regimes.

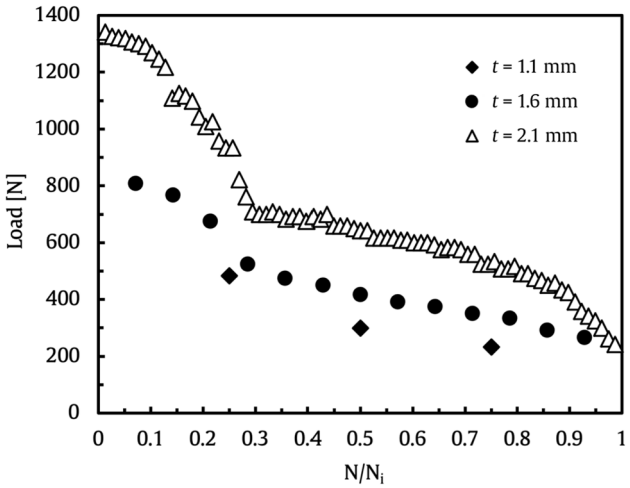

Fig. 11. Evolution of impact load for different thicknesses.

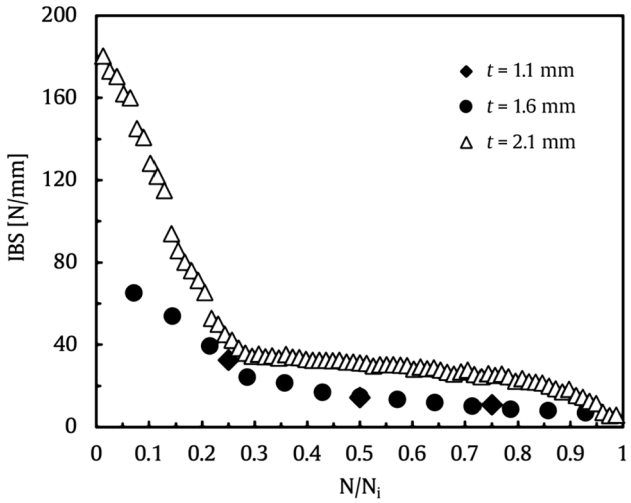

Fig. 13. Evolution of the impact bending stiffness for different thicknesses.

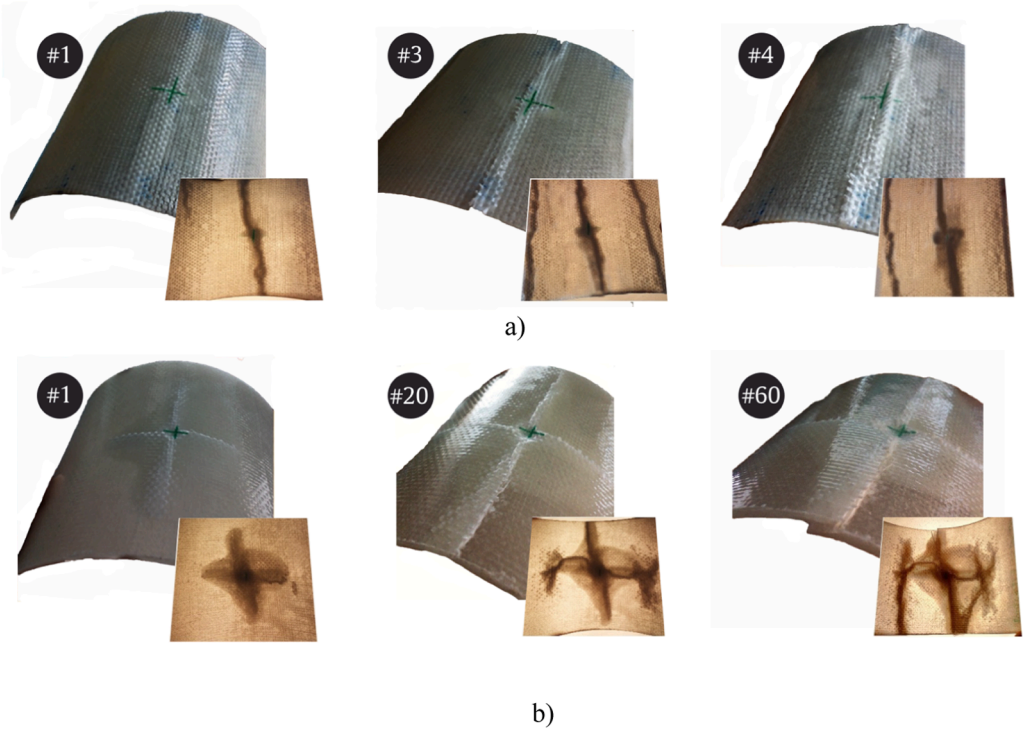

Fig. 14. Evolution of damage mechanisms as function of impact numbers: a) $t = 1.1$ mm; b) $t = 2.1$ mm.

On the other hand, and according to the literature [29,46], impact bending stiffness (IBS) and damage severity (damage area) are directly related, although the regimes that describe the evolution of each parameter are inverse. To prove this evidence, Fig. 14 shows some photos of the damage evolution related to shells with thicknesses of 1.1 mm and 2.1 mm subjected to damage multi-impacts, and the damage severity measured by the residual compressive strength shown in Fig. 15. Residual strength was evaluated only, as an example, for shells with a thickness of 1.6 mm, whose total perforation (impact fatigue life) was reached between 12 and 14 impacts.

It is possible to observe a strong dependence of the residual strength with the number of impacts, which can be expressed by a bilinear model. Compared to the control specimens (not impacted), the residual strength abruptly decreases from 511.6 N to 230 N, which represents a decrease of around 55 %. In terms of impact performance, the previously reported decrease in static strength (55 %) occurs during the first 50 % of the impact fatigue life and, for the same fatigue life values, the impact load decreases by around 48.5 % (see Fig. 11). This analysis proves that the impact load represents the value that the composite can tolerate before undergoing major damage [25,30]. Regarding the second regime, which occurs between the sixth and tenth impact, the decrease in residual compressive strength is only 8.5 %, revealing that the damage propagates with much less severity than in the first regime. As previously mentioned, the second phase is essentially characterized by the saturation of the damages initiated in the previous phase, with an almost linear evolution with the number of impacts, followed by the third regime where the damages evolve abruptly until the final failure. All this evidence confirms that the evolution of the IBS reflects the evolution of damage severity very well and can be used as a damage assessment tool with very good reliability [28,29].

Finally, for a better understanding of the impact damage effect on

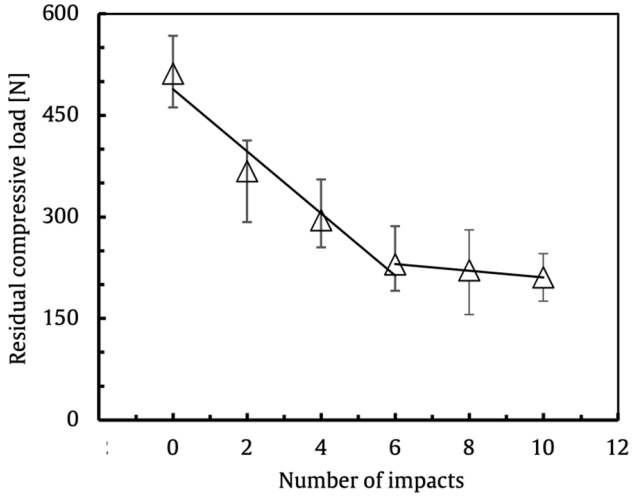

Fig. 15. Residual compressive load versus number of impacts.

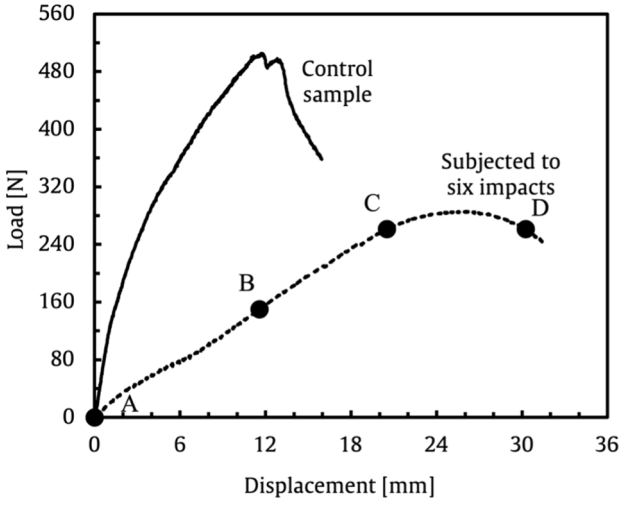

Fig. 16. Typical load–displacement curves for a control specimen and for one previously subjected to six impacts.

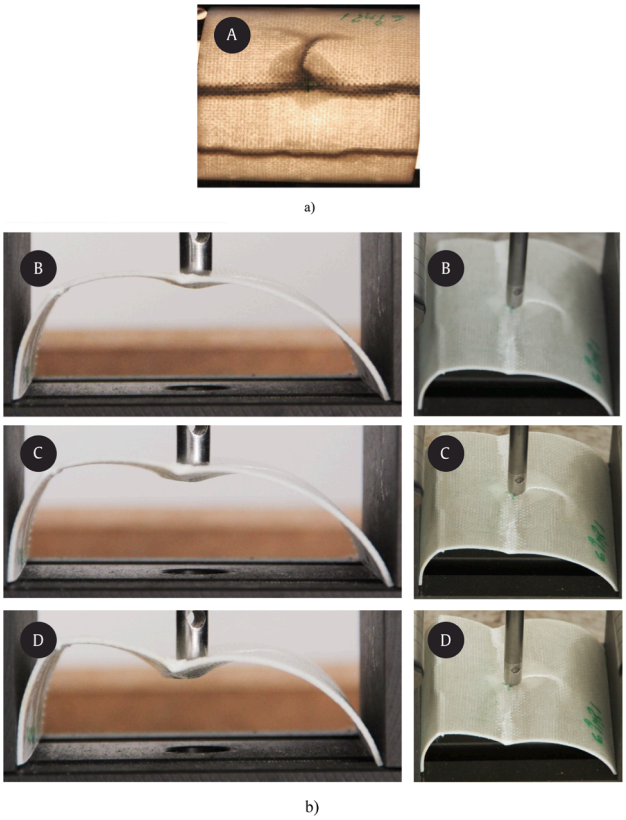

Fig. 17. a) Damage after six impacts; b) Damage for different values of compressive load.

residual compressive strength, Fig. 16 compares typical load–displacement curves for a control specimen and for one previously subjected to six impacts (corresponding to 50 % of the impact fatigue life). Fig. 17 shows the damage evolution for different load levels (A, B, C and D) represented in the load–displacement curve of the impacted specimen in Fig. 16.

Defining stiffness as the slope of the initial linear region of load–displacement curves, it is possible to confirm that after six impacts its value is significantly lower than the value observed for the control samples, as well as the compressive strength. In terms of average values, the decrease is around 77 % and 55 %, respectively, due to the damage caused by the impacts. In terms of damage progression, Fig. 17, it is very similar to that observed in the static tests described above, despite the propagation being much faster due to the damage introduced by impacts.

4. Conclusions

In this study, the thickness effect on semicylindrical E-glass woven fabric/polyester composite laminates was analysed and, for this purpose, low-velocity impact and static compressive tests were performed on specimens with three different thicknesses.

In terms of static performance, it was possible to conclude that higher thickness values are responsible by higher collapse loads and stiffness of the shells. The difference between the thinnest and thickest shells is about 252.6 %. Based on experimental results, it was possible to establish a mathematical equation capable of predicting the compressive strength as a function of thickness.

Regarding the impact response, increasing the thickness leads to higher stiffness and, consequently, to a higher impact load but less displacement and contact time. It was also found that the impact load and displacement have a linear response with increasing thickness, while the IBS is based on a second-degree polynomial. Moreover, increasing thickness leads to less severe damage because energy is dissipated by more interfaces. Finally, it was possible to observe that increasing the thickness leads to longer impact fatigue lives, reaching differences between the thinnest and thickest shells of 17.4 times, which can be explained by the different damage mechanisms developed in each configuration.

CRediT authorship contribution statement

P.N.B. Reis: Supervision, Conceptualization, Methodology, Writing – review & editing. **P. Sousa:** Data curation, Visualization, Investigation. **L.M. Ferreira:** Supervision, Writing – original draft, Writing – review & editing. **C.A.C.P. Coelho:** Investigation, Visualization.

Declaration of Competing Interest

The authors declare that they have no known competing financial interests or personal relationships that could have appeared to influence the work reported in this paper.

Data availability

Data will be made available on request.

Acknowledgments

This research is sponsored by national funds through FCT—Fundação para a Ciência e a Tecnologia, under the project UIDB/00285/2020.

References

[1] Her S-C, Liang Y-C. The finite element analysis of composite laminates and shell structures subjected to low velocity impact. Compos Struct 2004;66(1-4):277–85.
[2] Ying Y. Analysis of impact thresold energy for carbon fibre and fabric reinforced composites. J Reinf Plast Compos 1998;17(12):1056–75.
[3] Choi HY, Downs RJ, Chang F-K. A new approach toward understanding damage mechanisms and mechanics of laminated composites due to low-velocity impact: part I—experiments. J Compos Mater 1991;25(8):992–1011.
[4] Gong SW, Toh SL, Shim VPW. The elastic response of orthotropic laminated cylindrical shells to low-velocity impact. Compos Eng 1994;4(2):247–66.
[5] Richardson MOW, Wisheart MJ. Review of low-velocity impact properties of composite materials. Compos Part Appl Sci Manuf 1996;27:1123–31. https://doi.org/10.1016/1359-835X(96)00074-7.
[6] Olsson R. Low-and medium-velocity impact as a cause of failure in polymer matrix composites. Fail. Mech. Polym. Matrix Compos.: Elsevier; 2012. p. 53–78.
[7] Olsson R. Analytical prediction of damage due to large mass impact on thin ply composites. Compos Part Appl Sci Manuf 2015;72:184–91.
[8] Saghafi H, Brugo T, Zucchelli A, Fragassa C, Minak G. Comparison of the effect of preload and curvature of composite laminate under impact loading. FME Trans 2016;44(4):353–7.
[9] Imielińska K, Castaings M, Wojtyra R, Haras J, Le Clezio E, Hosten B. Air-coupled ultrasonic C-scan technique in impact response testing of carbon fibre and hybrid: glass, carbon and Kevlar/epoxy composites. J Mater Process Technol 2004;157:513–22.
[10] de Moura MFSF, Marques AT. Prediction of low velocity impact damage in carbon–epoxy laminates. Compos Part Appl Sci Manuf 2002;33(3):361–8.
[11] Choi IH. Low-velocity impact response analysis of composite pressure vessel considering stiffness change due to cylinder stress. Compos Struct 2017;160:491–502.
[12] Davies GAO, Olsson R. Impact on composite structures. Impact on compos struct Aeronaut J 2004;108(1089):541–63.
[13] Olsson R. Analytical model for delamination growth during small mass impact on plates. Int J Solids Struct 2010;47(21):2884–92.
[14] Krishnamurthy KS, Mahajan P, Mittal RK. A parametric study of the impact response and damage of laminated cylindrical composite shells. Compos Sci Technol 2001;61(12):1655–69.
[15] Kistler LS, Waas AM. Experiment and analysison the response of curved laminated composite panels subjected to low velocity impact. Int J Impact Eng 1998;21(9):711–36.
[16] Zhao GP, Cho CD. Damage initiation and propagation in composite shells subjected to impact. Compos Struct 2007;78(1):91–100.
[17] Arachchige B, Ghasemnejad H, Augousti AT. Theoretical approach to predict transverse impact response of variable-stiffness curved composite plates. Compos Part B Eng 2016;89:34–43.

[18] Krishnamurthy KS, Mahajan P, Mittal RK. Impact response and damage in laminated composite cylindrical shells. Compos Struct 2003;59(1):15–36.
[19] Cho C, Zhao G. Dynamic response and damage of composite shell under impact. KSME Int J 1999;13(9):596–608.
[20] Kumar S. Analysis of impact response and damage in laminated composite shell involving large deformation and material degradation. J Mech Mater Struct 2008; 3:1741–56.
[21] Kistler L. Experimental investigation of the impact response of cylindrically curved laminated composite panels. 35th Struct. Struct. Dyn. Mater. Conf., American Institute of Aeronautics and Astronautics; 1994. p. 2292–7.
[22] Olsson R. Mass criterion for wave controlled impact response of composite plates. Compos Part Appl Sci Manuf 2000;31(8):879–87.
[23] Amaro AM, Reis PNB, Magalhães AG, de Moura MFSF. The Influence of the boundary conditions on low-velocity impact composite damage. Strain 2011;47: e220–6. https://doi.org/10.1111/j.1475-1305.2008.00534.x.
[24] Campos Pais Coelho CA, Navalho FVP, Reis PNB. Impact response of laminated cylindrical shells. Frat Ed Integrità Strutt 2019;13:411–8. https://doi.org/10.3221/IGF-ESIS.48.39.
[25] Reis PNB, Coelho CACP, Navalho FVP. Impact response of composite sandwich cylindrical shells. Appl Sci 2021:11. https://doi.org/10.3390/app112210958.
[26] Ferreira, L. Coelho, C. Reis, P. Impact Response of Semi-Cylindrical Composite Laminate Shells Under Repeated Low-Velocity Impacts. 2022 Adv. Sci. Eng. Technol. Int. Conf. ASET, 2022, p. 1–5. https://doi.org/10.1109/ASET53988.2022.9735043.
[27] Silva MP, Santos P, Parente JM, Valvez S, Reis PNB, Piedade AP. Effect of post-cure on the static and viscoelastic properties of a polyester resin. Polymers 2020:12. https://doi.org/10.3390/polym12091927.
[28] David-West OS, Nash DH, Banks WM. An experimental study of damage accumulation in balanced CFRP laminates due to repeated impact. Compos Struct 2008;83(3):247–58.
[29] Amaro AM, Reis PNB, Neto MA, Louro C. Effects of alkaline and acid solutions on glass/epoxy composites. Polym Degrad Stab 2013;98(4):853–62.
[30] Reis PNB, Ferreira JAM, Santos P, Richardson MOW, Santos JB. Impact response of Kevlar composites with filled epoxy matrix. Compos Struct 2012;94(12):3520–8.
[31] Reis P, Ferreira J, Zhang Z, Benameur T, Richardson M. Impact response of Kevlar composites with nanoclay enhanced epoxy matrix. Compos Part B Eng 2013;46: 7–14.
[32] Andrew JJ, Arumugam V, Saravanakumar K, Dhakal HN, Santulli C. Compression after impact strength of repaired GFRP composite laminates under repeated impact loading. Compos Struct 2015;133:911–20.
[33] Schoeppner GA, Abrate S. Delamination threshold loads for low velocity impact on composite laminates. Compos Part Appl Sci Manuf 2000;31(9):903–15.
[34] Belingardi G, Vadori R. Low velocity impact tests of laminate glass-fiber-epoxy matrix composite material plates. Int J Impact Eng 2002;27(2):213–29.
[35] Gómez-del Río T, Zaera R, Barbero E, Navarro C. Damage in CFRPs due to low velocity impact at low temperature. Compos Part B Eng 2005;36(1):41–50.
[36] Reis P, Santos P, Ferreira J, Richardson M. Impact response of sandwich composites with nano-enhanced epoxy resin. J Reinf Plast Compos 2013;32:898–906. https://doi.org/10.1177/0731684413478993.
[37] Amaro AM, Reis PNB, de Moura MFSF, Neto MA. Influence of open holes on composites delamination induced by low velocity impact loads. Compos Struct 2013;97:239–44. https://doi.org/10.1016/j.compstruct.2012.09.041.
[38] García-Castillo SK, Sánchez-Sáez S, Barbero E. Influence of areal density on the energy absorbed by thin composite plates subjected to high-velocity impacts. J Strain Anal Eng Des 2012;47:444–52. https://doi.org/10.1177/0309324712454996.
[39] Arachchige B, Ghasemnejad H. Post impact analysis of damaged variable-stiffness curved composite plates. Compos Struct 2017;166:12–21. https://doi.org/10.1016/j.compstruct.2017.01.018.
[40] Amaro AM, Reis PNB, Neto MA. Experimental study of temperature effects on composite laminates subjected to multi-impacts. Compos Part B Eng 2016;98:23–9. https://doi.org/10.1016/j.compositesb.2016.05.021.
[41] Amaro AM, Reis PNB, de Moura MFSF, Neto MA. Multi-impact response of composite laminates with open holes. Polym Compos 2018;39:2490–8. https://doi.org/10.1002/pc.24235.
[42] Coelho SRM, Reis PNB, Ferreira JAM, Pereira AM. Effects of external patch configuration on repaired composite laminates subjected to multi-impacts. Compos Struct 2017;168:259–65. https://doi.org/10.1016/j.compstruct.2017.02.069.
[43] Azouaoui K, Rechak S, Azari Z, Benmedakhene S, Laksimi A, Pluvinage G. Modelling of damage and failure of glass/epoxy composite plates subject to impact fatigue. Int J Fatigue 2001;23:877–85. https://doi.org/10.1016/S0142-1123(01)00050-0.
[44] Reis PNB, Neto MA, Amaro AM. Multi-impact behaviour of composite laminates under constant and different energy levels. Compos Struct 2022;294:115788. https://doi.org/10.1016/j.compstruct.2022.115788.
[45] Santos RAM, Reis PNB, Santos MJ, Coelho CACP. Effect of distance between impact point and hole position on the impact fatigue strength of composite laminates. Compos Struct 2017;168:33–9. https://doi.org/10.1016/j.compstruct.2017.02.045.
[46] Amaro A, Reis P, Neto M, Louro C. Effect of different acid solutions on glass/epoxy composites. J Reinf Plast Compos 2013;32:1018–29. https://doi.org/10.1177/0731684413483886.